Mechanical and Microstructural Evolution of Solid Graphite Rocket Nozzle Throats in Extreme Temperature and Pressure Conditions

Burçin Kaygusuz[1], Barış Nigar[2,3], Levent Ünlüsoy[3], Demirkan Çöker[4], Sezer Özerinç[1,2]

[1]Middle East Technical University, Department of Micro and Nanotechnology, Ankara, Turkey
[2]Middle East Technical University, Department of Mechanical Engineering, Ankara, Turkey
[3]Roketsan Missile Industries Inc., Ankara, Turkey
[4]Middle East Technical University, Department of Aerospace Engineering, Ankara, Turkey

Abstract

Durability of the rocket nozzle and the throat component is one of the key aspects for the reliable operation of a rocket during its trajectory. Graphite is commonly used as a throat material due to its high temperature resistance, ablative characteristics and low cost. However, graphite can fracture due to the combined effects of thermal loading and pressure during rocket firing, which is catastrophic for the operation of the rocket. Therefore, there is a need to understand all aspects of graphite failure, which will enable the more reliable design of the throat. In this work, we investigated the changes to the microstructural and mechanical properties of graphite upon its testing in an actual motor in static firing configuration. The results indicate that for the operation of the graphite throat in the actual combustion environment up to 3 seconds, the throat microstructure does not change considerably. On the other hand, nanoindentation measurements indicate considerable hardening upon firing, which suggests an embrittlement undesirable for the reliable operation of the throat. The results emphasize the importance of longer exposure times for the characterization of fracture and related effects.

1. Introduction

Graphite is a commonly used material in rocket nozzle throats owing to its high resistance to ablation in extreme environments combined with good machinability and cost effectiveness [1,2]. Combination of high pressure, temperature, and the oxidation caused by the exhaust products result in the initiation and propagation of cracks on the throat surface, which is a major challenge for the reliable operation of the rocket [3]. In this study, we investigated the changes to the microstructural and mechanical properties of graphite before and after testing in a motor in static firing mode. X-Ray Diffraction (XRD) for phase identification and crystalline structure, X-Ray Fluorescence Spectrometry (XRF) for elemental analysis, and Raman Spectroscopy for understanding the bonding characteristics were utilized. Optical and scanning electron microscopy (SEM) helped to understand the morphology of graphite before and after testing.

2. Experimental Procedure

Graphite used in the throat material is an isomolded dense electrographite with porosity level of 9%. Before performing the motor tests, characterization was performed on rectangular graphite plates with dimensions 10 × 3 × 0.5 cm. In this discussion, "graphite plates" will refer to these machined specimens from molded graphite, without any motor testing. In addition to the study of the as-molded graphite, graphite nozzles were tested in an actual test motor in static firing conditions with a characteristic heat flux profile for 3 seconds using a solid propellant. After the testing, the throat was removed, radially cut, and the cross-sections were polished for microstructural characterization and nanoindentation testing. These specimens will be referred as "fired graphite".

A Rigaku Ultima IV X-ray diffractometer using a θ-2θ geometry analyzed the samples for its crystal structure and phases. Dispersive Raman Spectroscopy verified the chemical structure of graphite with a laser wavelength of 532 nm. X-ray fluorescence (XRF) (Rigaku ZSX Primus II) quantified the chemical composition of the graphite samples. An FEI QUANTA 400F Field Emission scanning electron microscope (SEM) analyzed the morphology of the graphite surface.

To understand the mechanical behavior of graphite, uniaxial compression and nanoindentation were performed on the same batch of the graphite plates used for the microstructural characterization. A Zwick Z020 uniaxial testing system compressed cylindrical specimens of graphite. Two types of cylinders with 10 and 20 mm diameter both having a height of 20 mm were tested. All compression samples were cut from as-molded pieces of graphite without firing. Measurements were repeated on 6 samples for each geometry. The displacement rate was 0.1 mm/min.

An Agilent G200 nanoindenter performed nanoindentation tests on graphite plates, and also on the cross sections of the fired graphite nozzle. By performing nanoindentation at different locations over the cross section, we examined possible changes in local mechanical properties due to heating and pressure effects.

3. Results and Discussion

XRF results (spectrum not shown) has shown that specimens are composed mostly of graphite as expected. The plates are 96.7 wt.% carbon and 3.2 wt.% oxygen with other small impurities of Si, S, Ca, Mg and Al all below 0.02%.

Figure 1 shows X-ray diffraction and Raman spectra of graphite plates and fired graphite. The results from the two samples are mostly coincident considering the uncertainties associated with the specimens and the measurements. This indicates that there is no major change in the chemistry and microstructure of graphite upon testing. XRD results show that the crystal structure of graphite is hexagonal and all peaks belong to the Graphite-2H phase, in agreement with the ICSD PDF data (00-041-1487). The most common features in the Raman spectra are labeled in Figure 1(b). In this figure, D and G bands are characteristic peaks for graphite. The dominant G band comes from the sp^2 vibrations [4].

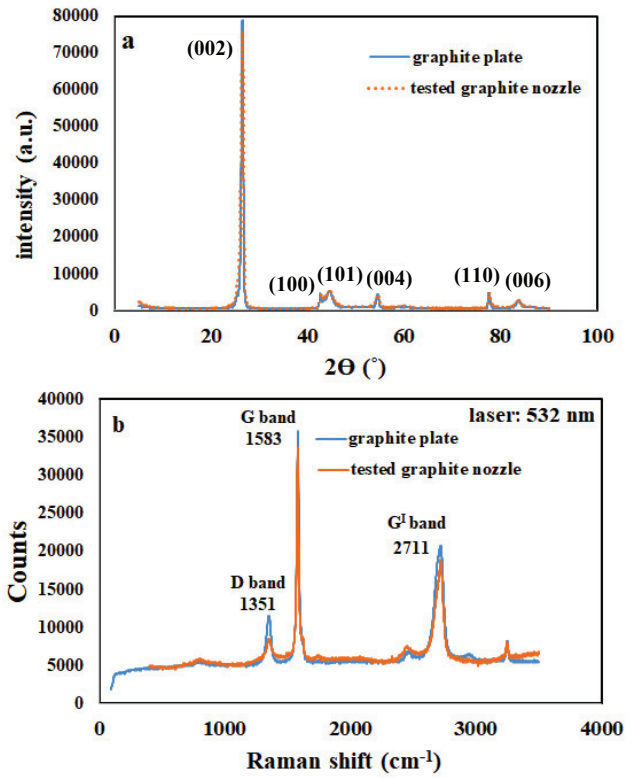

Figure 1. (a) XRD spectrum and (b) Raman spectrum of graphite plates and fired graphite.

Figure 2 shows SEM images of graphite plate and fired graphite. In fired graphite, regions with higher brightness are observed. We attributed this to the sticking of the fuel particles to the nozzle, potentially abrading and oxidizing the surface of the nozzle. EDS analysis to be done will provide further insight to the surface characteristics.

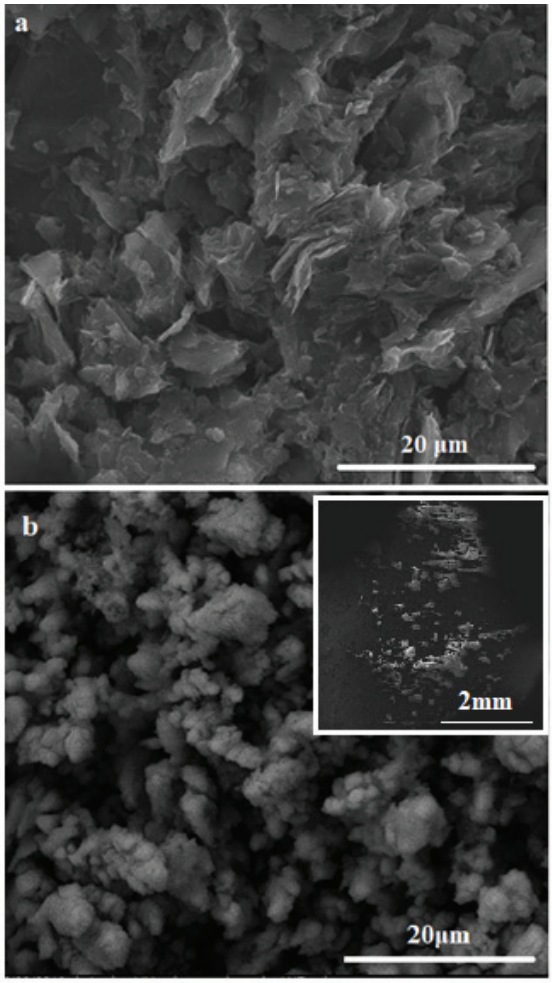

Figure 2. SEM images of (a) graphite plate, and (b) fired nozzle graphite. Inset of (b) shows a low magnification view of the brighter regions.

Figure 3 shows twp 20 mm diameter, 20 mm height test specimens before and after compression. The specimens failed in a brittle fashion and most specimens fragmented into multiple pieces upon testing as shown in the figure. Figure 4 shows the stress-strain behavior of 10 mm diameter and 20 mm diameter specimens. Overall the results have good repeatability, considering the fact that in brittle samples the variance is usually high.

Table 1 summarizes the compression test results in terms of the average values and standard deviations. The 10 mm

diameter specimens have an average compressive strength of 56 MPa. Previous measurements on graphite indicated strength values around 60-70 MPa under compression [3,5]. Considering that the results are highly dependent on the manufacturing details and porosity of the specimens for brittle materials, the discrepancy is within reasonable limits. Larger diameter samples have a slightly higher strength, which might be due to the better alignment of these samples with respect to the loading surfaces. Furthermore, the standard deviation of the compressive strength is lower for this larger-diameter batch.

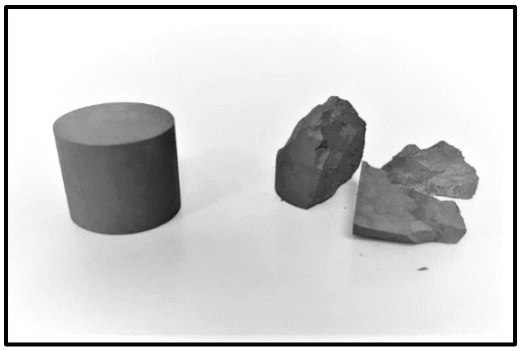

Figure 3. Two 20 mm-diameter compression test specimens, untested on the left, and after compression testing on the right.

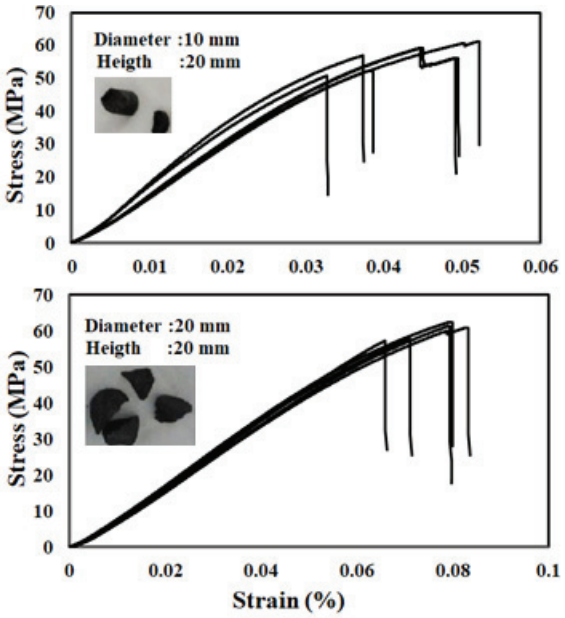

Figure 4. Results of compression tests of graphite cylinders cut from graphite plates with two different diameters.

Table 1. Summary of Compression testing results.

Sample Diameter	Average Compressive Strength (MPa)	Standard Deviation (MPa)
10 mm	56.1	3.7
20 mm	59.6	1.9

In addition to compression tests, nanoindentation was performed at various locations over the cross section of the fired graphite. At least 15 indentations were performed on each selected location on the sample and the average results are summarized in Table 2.

Nanoindentation results show that the hardness and the elastic modulus of the graphite dramatically increase upon firing. The increase is significantly higher than the hardness deviations within a sample, indicating that firing actually affects the mechanical properties at the small scale. This hardening is observed at different locations over the cross-section of the fired graphite, including regions relatively farther away from the firing. This suggests that the hardening might be related to the temperature rise and associated morphology change in graphite. The throat component reaches to very high temperatures as a whole upon firing, and its effect on the mechanical properties would appear throughout the cross-section. Additional experiments with longer firing times and more detailed mechanical mapping by using nanoindentation will provide further insight to the observed hardening.

Table 2. Nanoindentation results of graphite samples

Sample	Hardness (GPa)	σ_H (GPa)	Elastic Modulus (GPa)	σ_E (GPa)
graphite plate	0.31	0.07	9.1	1.2
fired graphite	0.51	0.05	12.4	1.3

4. Conclusions

In this work, we investigated the microstructural and mechanical properties of graphite used in rocket nozzles in as-molded state and after testing in static firing mode. After 3-second firing experiments, there was no significant change in the microstructure and chemistry of graphite. However, significant hardening was observed through nanoindentation experiments. Possible embrittlement accompanied by this hardening might be critical for the reliable operation of the nozzle for longer firing times.

Future studies will focus on compression testing of fired graphite, and microstructural and mechanical characterization of graphite tested for longer firing periods.

Acknowledgements

We would like to thank Roketsan Laboratories and machine shop for testing and manufacturing of the specimens, METU Central Laboratory, METU Mechanical

Engineering Mechanical Testing Laboratory, and Koç University KUYTAM for their contributions in the characterization experiments. We would like to thank Servet Şehirli for his help with the mechanical testing and data interpretation.

References

[1] J. R. Johnston, R. A. Signorelli, and J. C. Freche, Performance of Rocket Nozzle Materials with Several Solid Propellants, NASA, 1966, Cleveland, USA.
[2] R. Acharya, and K. K. Kuo, Journal of Propulsion and Power, 23 (2007) 1242–1254.
[3] J. H. Kim, Y. S. Lee, D. H. Kim, N. S. Park, J. Suh, J. O. Kim, and S. Il Moon, Materials Science and Engineering: A, 387–389 (2004) 385–389.
[4] S. Reich, and C. Thomsen, Philosophical Transactions of the Royal Society of London A: Mathematical, Physical and Engineering Sciences, 362 (2004) 2271–2288.
[5] H. Choi, J. Kim, Y. Kim, B. Seo, and S. Moon, Journal of the Korean Society of Propulsion Engineers, 18 (2014) 61–66.